Modelling two-dimensional chloride diffusion in repaired RC structures for sustainable maintenance management

Quynh Truong, Charbel-Pierre El Soueidy, Lara Hawchar, Yue Li, Emilio Bastidas-Arteaga

Please cite this paper as: Truong QC, El Soueidy C-P, Hawchar L, Li Y, Bastidas-Arteaga E. (2023). Modelling two-dimensional chloride diffusion in repaired RC structures for sustainable maintenance management. Structures, 51:895–909. https://doi.org/10.1016/j.istruc.2023.03.088

Modelling Two-Dimensional Chloride Diffusion in Repaired RC Structures for Sustainable Maintenance Management

Quynh Chau Truong[1,2], Charbel-Pierre El Soueidy[1], Lara Hawchar[3], Yue Li[4], Emilio Bastidas-Arteaga[5]

[1] Institute for Research in Civil and Mechanical Engineering (GeM - UMR 6183), Université de Nantes, Nantes, France
[2] Faculty of Project Management, The University of Danang – University of Science and Technology, Danang, Viet Nam
[3] Discipline of Civil, Structural and Environmental Engineering, School of Engineering, University College Cork, Cork, Republic of Ireland
[4] Department of Civil and Environmental Engineering, Case Western Reserve University, Cleveland, Ohio 44106, USA
[5] Laboratory of Engineering Sciences for the Environment (LaSIE - UMR CNRS 7356), La Rochelle University, La Rochelle, France

*Corresponding author: Emilio Bastidas-Arteaga
Phone: +33 (0)5 86 56 22 32, email: ebastida@univ-lr.fr

Abstract

Both public and private infrastructure management agencies are responsible for chloride-related corrosion damage to coastal reinforced concrete (RC) structures, which often requires extensive repairs. These repairs are intended to provide serviceability and safety while reducing costs and environmental impact. While there are many repair methods, techniques, and materials available, little is known about their long-term performance and durability. This study examines two-dimensional chloride ingress into square cross section RC columns and their durability using cover replacement techniques with several shapes, thicknesses, locations, and repair times. First, a two-dimensional repair model is developed to simulate these repair strategies and predict their serviceability performance. Two orthogonal concrete replacement strategies (OCR1 and OCR2) and one circular concrete replacement strategy (CCR3) are studied. Next, a method to evaluate and compare maintenance strategies in terms of durability, cost, and environmental impact is also considered. The results of this study reveal that the corners of a column are the most critical areas to evaluate chloride concentration when predicting the time of corrosion initiation and estimating repair time. For long-term maintenance management, the circular concrete replacement strategy is recommended over orthogonal concrete replacement for repair of RC columns exposed to chloride-induced corrosion. The CCR3 strategy requires fewer repairs and achieves higher cost-effectiveness and sustainability compared to the other strategies.

Key words: chloride ingress; reinforced concrete; corrosion; two-dimensional model; repair strategy; concrete replacement; sustainability.

1 Introduction

Chloride-induced corrosion has a significant impact on the durability of RC structures in coastal areas. The penetration of chloride ions from the environment into concrete cover and reinforcement is influenced by exposure conditions, weather elements, quality of materials, and construction practices [1,2]. This process can be divided into two phases: initiation and propagation. The propagation phase is much shorter than the initiation phase. So, the service life of a structure is defined as the period between the original condition and the onset of corrosion. Corrosion is considered onset when the chloride concentration deposited on the surface of the reinforcing bars reaches a certain threshold (defined as the critical chloride content or C_{crit}) and dissolves a passive protective film on the steel bars [3].

Concrete structures are supposed to have a high tolerance to deterioration over a long period of time (50 to 100 years). However, many construction projects, especially those in aggressive marine environments, have experienced premature corrosion and subsequent deterioration in strength and serviceability of their RC structural elements [4]. Maintenance and repair works are therefore undertaken to extend the safety and service life of such structures. These maintenance activities should be performed before or as soon as corrosion begins [5] to reduce failure risks. There are several repair methods, such

as replacing concrete cover or increasing the concrete coating or cathodic protection [6–8]. The cover rebuilding or cover replacement method is particularly common among them. It removes the chloride-contaminated concrete and rehabilitates the structure by placing new concrete or repair mortar without damaging the reinforcement bars. The new material is typically placed as wet shotcrete, dry shotcrete, formed concrete, or by manual repair [8]. Building a credible model to assess the degree of corrosion and predict the service life of RC structures with repairs is a challenging task that has become crucial for engineers to enable proper condition monitoring and appropriate retrofitting [5,9,10].

Recent research has focused on modeling chloride transport in repaired concrete members and determining repair times over the life of a structure. It was found that the mechanism of chloride diffusion into two concrete layers (repair material and original aged concrete) consists of chloride penetration from the exposed concrete surface and distribution of chloride ions remaining in the aged concrete [11,12]. In the method of cover rebuilding, the material compatibility and the depth of concrete replacement are the two critical factors that can affect the effectiveness of the maintenance measures [13,14]. These issues have been discussed in previous research, but the scope of the studies was largely limited to a one-dimensional (1D) model of chloride ingress and has not yet been applied to the two-dimensional problem that concerns several structural components in practice [9,14,15]. For example, the corners and edges of crossbeams, square piles and columns, or rectangular concrete structures, are often exposed to two-dimensional (2D) chloride diffusion [16,17]. In these cases, the use of 1D chloride diffusion models underestimates the chloride concentration at the critical locations of concrete structures, thereby overestimating the time for corrosion initiation. Therefore, accurate prediction of the service life of marine RC components to be repaired requires the use of 2D chloride-induced corrosion models, especially for modelling corners and edges in the concrete components.

Recently, several 2D numerical models have been developed to estimate the chloride distribution in concrete based on finite element method and finite difference method. Among them, Ying et al. [18] proposed a model using a constant chloride diffusion coefficient and neglecting the time variation of this parameter due to concrete aging. Hu et al. [19] established 1D and 2D models for time-dependent chloride diffusion that considered the effects of temperature, relative humidity, and a time aging factor of concrete. More comprehensive models were developed for various exposure conditions that considered the diffusion-convection coupling system during chloride penetration, seasonal variations in humidity and heat transfer, time-dependent surface boundary, concrete aging, and chloride binding capacity [20–24]. Although many scientists have conducted extensive research on the 2D model of chloride ingress, the available studies have not yet considered repairs and their response to these maintenance actions during the life of a structure. Indeed, there is little information on the underlying mechanisms of 2D chloride transport in repaired concrete structures and their long-term performance after periodic repairs. Moreover, these repairs need to be optimized for maximum serviceability and safety while reducing costs and environmental impacts [1,25]. There have been several studies that have calculated the cost of multiple repairs over the life of the structure [26,27] or estimated the environmental impact of repair and maintenance activities [25]. However, there has not been a comprehensive study that focuses on defining different repair strategies, evaluating their effectiveness, and thoroughly comparing these solutions based on economic and environmental considerations, such as maintenance cost, CO_2 emission and waste generation.

The aim of this study is to propose a methodology for service life assessment and sustainable maintenance management for repaired RC elements (columns, beams) located in a marine environment. A 2D numerical model is developed in FreeFem++, which combines finite element and finite difference methods to solve constitutive nonlinear partial differential equations of chloride diffusion processes in existing and repaired concrete. The evolution of chloride concentration in the corner and edge regions of concrete members is evaluated considering the effects of temperature, humidity, water-cement ratio, chloride binding capacity and concrete aging. Then, the kinetics of chloride ingress in repaired concrete are studied to develop a maintenance model that can simulate various repair measures and predict the extension of service life for repaired RC structures. The study is then performed for the maintenance procedures, where the reactive approach is first applied to perform the repair when the chloride content at the reinforcement cover depth exceeds a threshold. The proposed methodology is illustrated with three

concrete replacement strategies with different repair features (shape, thickness, location). Finally, a comparison framework that weighs the expected number of repairs, maintenance costs, and environmental impacts is proposed to evaluate the sustainability of each maintenance strategy.

The paper begins by describing the equations for chloride diffusion, then the numerical solution and experimental validation are presented (Section 2). Section 3 provides the 2D model of chloride distribution in repaired RC structures that is illustrated with an example. Section 4 focuses on sustainable maintenance management, followed by an example and discussion.

2 Two-dimensional chloride ingress model

2.1 Governing equations of chloride diffusion

Chloride penetration in marine RC structures is typically governed by chloride diffusion, convection, adsorption, permeation, and chloride binding, among other mechanisms. However, it has been shown that Fick's second law of diffusion serves to characterize the distribution of chloride content in concrete [3]. The simplification of the chloride transport mechanism to a diffusion-based model is reasonable and acceptable under the condition that RC structures operate in a marine environment that can generally be considered saturated in some exposure zones, e.g., the submerged zone [16,28–30]. Therefore, in this study, the governing equation for two-dimensional chloride transport in concrete is:

$$\frac{\partial C_{fc}}{\partial t} = D_c^* \left(\frac{\partial^2 C_{fc}}{\partial x^2} + \frac{\partial^2 C_{fc}}{\partial y^2} \right) \quad (1)$$

where C_{fc} (kg/m^3 concrete) is the chloride concentration at point (x, y) in a horizontal concrete cross-section at exposure time t (s), x (m) and y (m) are the distances from the exposure surface in the X and Y directions, respectively. D_c^* (m^2/s) represents the apparent chloride diffusion coefficient and is estimated as:

$$D_c^* = \frac{D_c}{1 + \left(\frac{1}{w_e}\right)\left(\frac{\partial C_{bc}}{\partial C_{fc}}\right)} \quad (2)$$

The relationship between free chloride and bound chlorides, $\partial C_{bc}/\partial C_{fc}$ is defined as chloride binding capacity, which can be formulated by the Langmuir binding isotherm:

$$C_{bc} = \frac{\alpha C_{fc}}{1 + \beta C_{fc}} \quad (3)$$

Considering temperature $f_1(T)$, concrete age $f_2(t)$, and relative humidity $f_3(h)$, the time-dependent chloride diffusion coefficient D_c in Eq. (1) is defined as:

$$D_c = D_{c,\,ref}\, f_1(T) f_2(t) f_3(h) \quad (4)$$

$$f_1(T) = \exp\left[\frac{U_c}{R}\left(\frac{1}{T_{ref}} - \frac{1}{T}\right)\right] \quad (5)$$

$$f_2(t) = \left(\frac{t_{ref}}{T}\right)^{m_c} \quad (6)$$

$$f_3(h) = \left[1 + \frac{(1-h)^4}{(1-h_c)^4}\right]^{-1} \quad (7)$$

The description of parameters used in 2D chloride ingress model, such as w_e, α, β, $D_{c,ref}$, U_c, R, T_{ref}, m_c, t_{ref}, and h_c, is shown in Table 1. The values of these parameters can be found in previous studies [20–23].

Table 1. Parameters used in the 2D chloride ingress model (sources: [20–23])

Parameter	Description	Unit	Value
w_e	Evaporable water content		0.1316
α	Binding constants		0.09
β			0.1185
$D_{c,ref}$	Reference chloride diffusion coefficient	m^2/s	3×10^{-11}
U_c	Activation energy of chloride transport	KJ/mol	41.8
R	Gas constant	J/ (mol K)	8.314
T_{ref}	Reference temperature	K	296

T	Absolute temperature	K	Depending on the external environmental conditions
m_c	Aging factor		0.15
t_{ref}	Reference time at which $D_{c,ref}$ is measured	days	28
h_c	Relative humidity at which D_c falls to half between its maximum and minimum values		0.75
h	Relative humidity inside the concrete		Depending on the external environmental conditions

2.2 Numerical modeling of chloride ingress

As shown in section 2.1, Eqs. (1)-(7) are used to characterize the process of corrosion initiation in RC structures subjected to chloride diffusion. The partial differential equations are solved in space and time using a 2D finite element model and finite difference direct integration method developed in FreeFEM++ [31]. In this study, partial scale modeling is used to build a truncated model for a concrete cover region in symmetrical boundary conditions (Fig. 1) [22,23], mainly to consider:

- the chloride concentration on the steel reinforcements embedded in different locations of the RC components;
- the complete chloride ingress 2D surfaces before/after repair; and
- the effect of the size and shape of the replacement concrete area.

Fig. 1 shows the 2D chloride ingress area of concrete to be modelled including the boundary conditions of the truncated chloride ingress model. In this study, to solve Eq. (1) with non-constant chloride diffusion coefficient, boundary conditions and initial conditions for 2D chloride ingress model are defined respectively, as below:

$$\begin{cases} C_{fc}(x,y,t)=C_{fc}^{s}, & \text{for } (x,y)\in \Gamma_1,\ t>0 \\ C_{fc}(x,y,t)=C_0, & \text{for } (x,y)\in \Gamma_2,\ t>0 \end{cases} \quad (8)$$

$$C_{fc}(x,y,t) = C_0, \text{ for } (x,y) \in \Omega,\ t = 0 \quad (9)$$

where C_{fc}^{s} represents the chloride content of exposed concrete, which rises fast in the early stages before stabilizing in the latter stages [32]. Moreover, in this study, Eq. (1) is used to model chloride transport in submerged or splash zone, where C_{fc}^{s} can be considered as a constant corresponding to an average chloride concentration during the structure lifetime or the chloride concentration of seawater [33]. Γ_1 is the boundary of exposure surface, Γ_2 contains the remaining parts of the boundary within concrete. C_0 is the initial chloride concentration within concrete and Ω denotes the domain of 2D chloride diffusion (as shown in Fig. 1b).

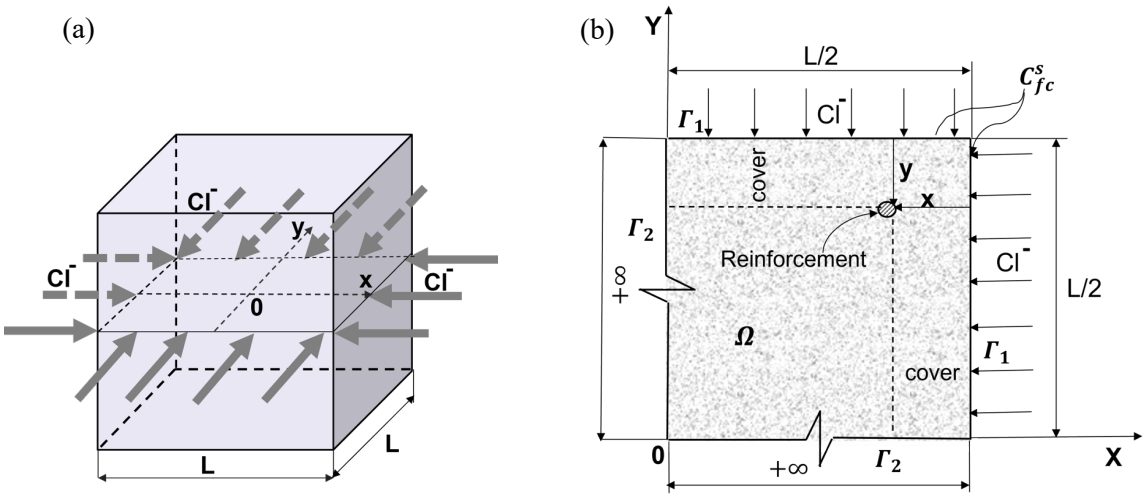

Fig. 1. (a) 2D chloride ingress area of concrete to be modelled, (b) Boundary conditions of a truncated chloride ingress model

2.3 Model validation

The numerical simulation in this paper is validated by comparison to the 2D chloride diffusion experiments conducted by Yu et al. [34]. In their work, 100 mm x 100 mm x 400 mm concrete cubes were immersed in an artificially saturated marine environment. After a curing period of 28 days at the temperature of 20ºC, four surfaces of the concrete were coated with epoxy resin, allowing chloride ions from the environment to penetrate onto the remaining two adjacent surfaces. The concrete samples were then placed in an automated simulation system and exposed to synthetic seawater. Experimental data on the distribution of chloride concentration were obtained by examining the chloride content from the corner and edge areas of the samples after 70- and 180-day exposure to the artificial marine environment. In order to ascertain the conditions in artificially simulated marine environment, a review of relevant experiments [28,35,36] was conducted to determine ambient temperature and relative humidity during testing. Generally, the samples are placed in controlled environmental conditions with a temperature of approximately 20°C and a relative humidity averaging 70% (ranging from 60-80%). Since the exact value is unknown, to validate the model, three different ambient temperatures (18°C, 20°C, and 23°C) and an average humidity value of 0.7 were utilized. The simulated chloride concentration was compared to the tested chloride results after 70 days (designated as M70-T18, M70-T20, M70-T23) and 180 days (designated as M180-T18, M180-T20, M180-T23) as depicted in Fig. 2. Even if these results are still based on assumptions, the agreement between the modeled chloride profile curves and the experimental chloride measurements indicates the validity of the chloride ingress model.

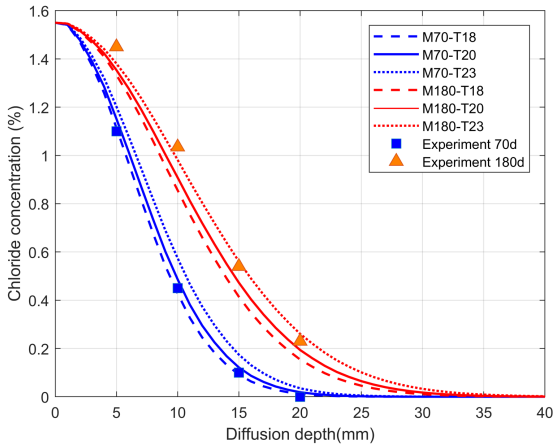

Fig. 2. Chloride diffusion model validation with data taken from **[34]**

The experimental work of Roy et al. [37] is also examined to validate the results of the numerical model. The concrete specimens were rectangular prisms with dimensions 100 mm x 100 mm x 500 mm. Data were obtained from the chloride penetration test of standard concrete after an 80-week exposure period in a submerged zone at a temperature of 20ºC and a relative humidity of 0.75. Fig. 3 shows the trend of free chloride distribution from FreeFEM++ modeling with the parameters used in the simulation. The comparison of the numerical modeling with previous experiments confirms the prediction accuracy of the model for 2D chloride ingress modelling.

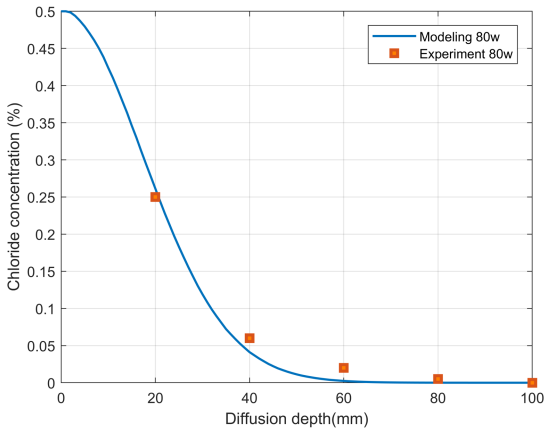

Fig. 3. Chloride diffusion model validation with data taken from **[37]**

3 Modeling of 2D chloride distribution in the repaired RC structures

3.1 Chloride ingress model considering repair

Over the past few years, there has been a significant amount of scientific research focused on investigating the kinetics of corrosion and modeling chloride distribution in repaired reinforced concrete (RC) structures [7,9,11–13,38]. Both experimental and in-situ observations, as well as numerical studies, have demonstrated that repaired concrete is subjected to two types of corrosion simultaneously: microcell corrosion (within a homogenous material) and macrocell corrosion (between two material layers). In addition to chloride penetration from the environment, concrete repair leads to the redistribution of residual chloride ions from the existing concrete to the new concrete due to differences in chloride content between the two layers, which results in macrocell corrosion. While various models have been proposed for simulating the consequences of these processes through one-dimensional chloride ingress, developing a 2D corrosion model that considers repair remains a challenge.

This current study takes a numerical approach to develop such a 2D model that considers a time- and space-domain dependent diffusion coefficient in two layers of material corresponding to old and repaired concrete. Fig. 4 illustrates the evolution of chloride transport in repaired RC structures in detail. The chloride profile before repair is shown in Fig. 4a with color iso-contour lines. Prior to cover renewal, the main source of chloride that penetrates the concrete over time is chloride ions from the external environment abutting the concrete surface. Eqs. (1)-(9) are used to model the 2D penetration of chloride. Throughout the concrete section, the initial chloride concentration is assumed to be zero, $(C_{fc})_0 = 0$, the initial diffusion coefficient is defined as $D_c^*(t)$.

When the chloride concentration in the depth of reinforcement reaches a critical level, it is necessary to use cover replacement methods in which the damaged concrete cover is removed to a certain thickness and replaced with a layer of chloride-free repair material. Fig. 4b illustrates the chloride profile in the concrete immediately after repair in the case where the entire concrete cover is replaced. The repaired concrete layer and the unrepaired remaining concrete are represented by Ω_1 and Ω_2, respectively. Following repair, a new life cycle assessment is conducted for the structure, with separate initial conditions and model parameters for Ω_1 and Ω_2. While the initial chloride content in the repaired material layer is zero, this in the old concrete is the residual chloride ions, which were not removed after repair. Additionally, the diffusion coefficient of the repair concrete, D_{rep}^*, and model parameters related to material properties are updated to reflect the new repair material and new concrete aging based on Eqs. (2)-(7), while the diffusion process in the old concrete is governed by the original model parameters.

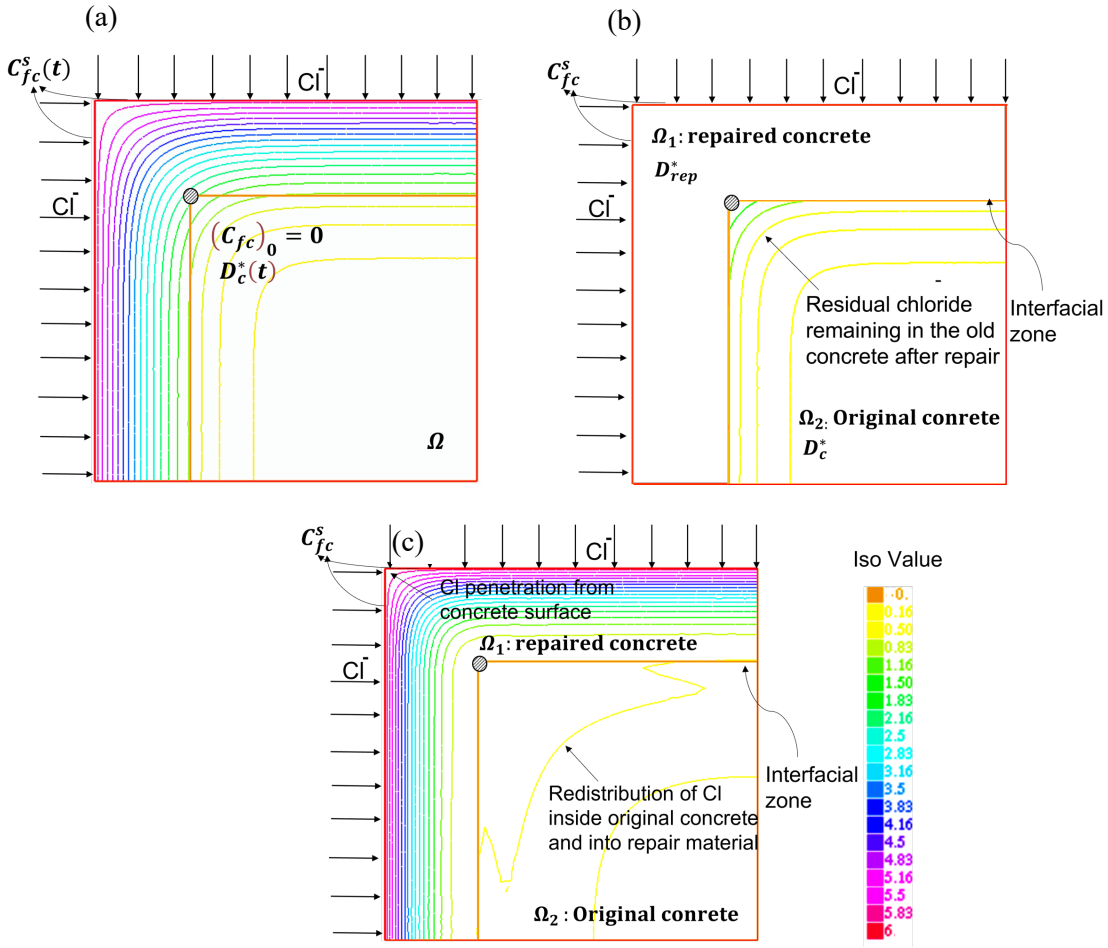

Fig. 4. (a) Chloride profile immediately before repair, (b) Chloride profile immediately after repair (c) Chloride profile after repair

Fig. 4c illustrates the chloride profile after repair. At this stage, there are two sources of chloride penetration: the exposed concrete surface to the chloride-rich environment and the residual chlorides presenting in the aged concrete. These residual chlorides will redistribute within Ω_2 (microcell corrosion) and diffuse through the interfacial area into Ω_1 (macrocell corrosion). As a result, simultaneous chloride ingress from these two sources of chloride ions will occur until reaching an equilibrium state. In the subsequent years, environmental chloride will be the sole source of chloride ions, resulting in a chloride profile similar to that depicted in Fig. 4a.

Due to the difference of the diffusion coefficients in two domains Ω_1 and Ω_2, the problem will involve a spatially domain-dependent diffusion coefficient after repair $D^*_{ar}(x, y, t)$:

$$D^*_{ar}(x,y,t)=\begin{cases} D^*_{rep}(t-\Sigma T^i_{ini}) & \text{if } (x,y)\in \Omega_1 \\ D^*_c(t) & \text{if } (x,y)\in \Omega_2 \end{cases} \quad (10)$$

where T^i_{ini} $(i = 1, 2\ldots n)$ is the time to corrosion initiation for a new service life assessment after i^{th} repairs. As a result, the partial differential equation based on Fick's diffusion law applied in this stage becomes:

$$\frac{\partial C_{fc}}{\partial t}=\left(\frac{\partial}{\partial x} D^*_{ar}(x,y,t)\frac{\partial C_{fc}}{\partial x}+\frac{\partial}{\partial y} D^*_{ar}(x,y,t)\frac{\partial C_{fc}}{\partial y}\right) \quad (11)$$

3.2 Numerical solution and modeling process in repaired concrete in FreeFem++

The FreeFEM++ program was utilized to address the issue of chloride diffusion in an existing and repaired RC structure [31]. FreeFEM++ is a free and open-source software that solves partial differential equations (PDEs) in 1D, 2D, and 3D boundary domains for nonlinear multiphysics systems. The software features a rapid interpolation procedure and a language for data manipulation across multiple meshes, reducing the number of source code lines required. The mesh is automatically generated in FreeFEM++, and the domain geometry is described through parametric equations of boundary segments.

The FreeFEM++ tool is suitable for predicting chloride penetration in concrete with regular repairs due to its use of independently measurable data as input, such as material properties and exposure environment, and its solution of the time evolution problem of chloride diffusion through the finite element method in space and finite differences in time. The tool also considers the nonlinear binding capacity between bound and free chlorides through a fast iterative procedure. Additionally, the tool can solve the problem of a two-layer concrete repair system using a domain decomposition technique, including iterative sub-structuring and connecting subdomains through interfacial conditions.

The modeling process of chloride diffusion in repaired concrete is shown in Fig. 5 as a flowchart of the numerical program in the FreeFEM++ software. The numerical structure must first be established through the formation of two subdomains, depending on the chosen repair strategy. The repair material and remaining concrete layers constitute the entirety of the concrete element, and the chloride concentration at critical locations is monitored. When the concentration reaches a threshold value for corrosion initiation, the repair is defined, and the repair material is considered with updated parameters. The calculation of a new service life for the structure is performed, taking into account the spatially domain-dependent and time-dependent diffusion coefficients of the two concrete domains. This process is repeated until the lifespan of the structure is reached, and the maintenance schedule corresponding to the repair strategy is determined through the timing of repairs.

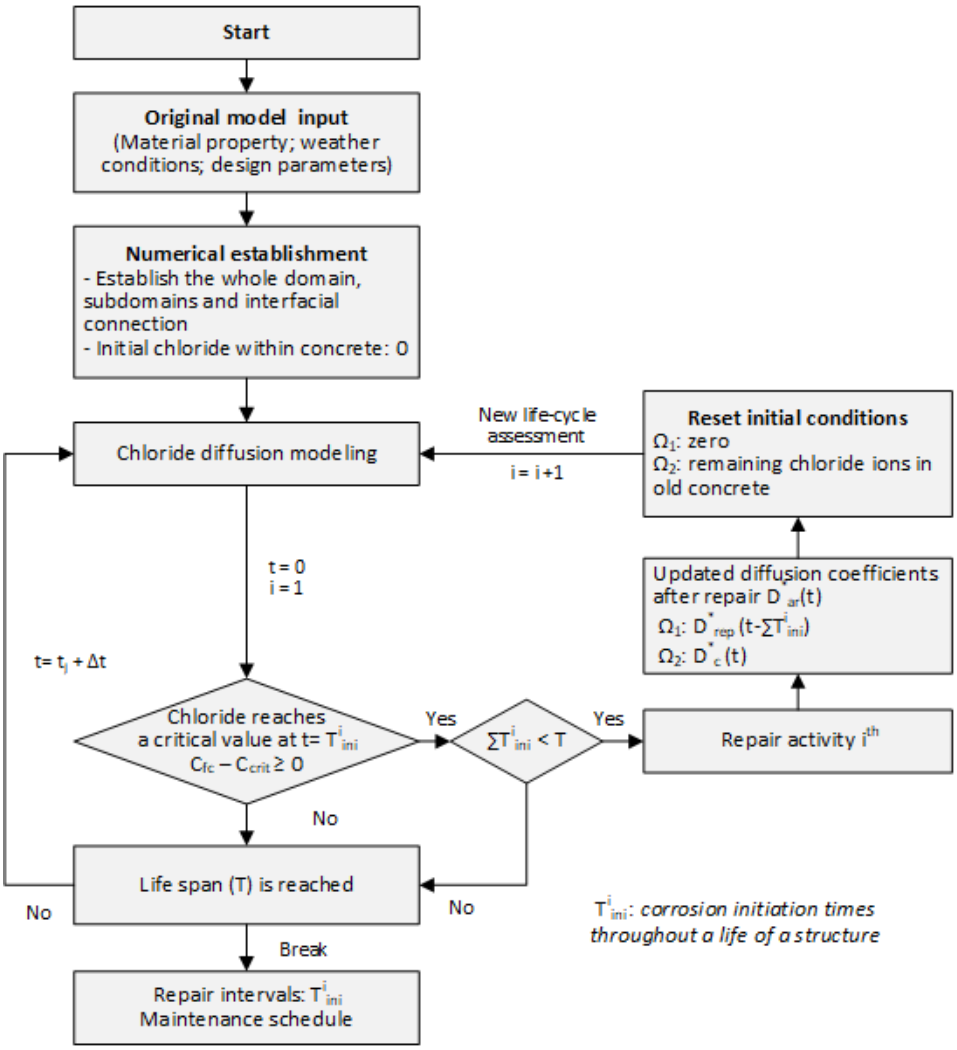

Fig. 5. Modeling process of chloride diffusion in repaired concrete

Therefore, FreeFEM++'s efficiency allows for the development of maintenance models with a wide range of cover rebuilding depths, repair times, and other repair parameters. The deterministic example in the following section demonstrates this in detail.

3.3 Illustrative example of a maintenance model

3.3.1 Problem description

Based on the analysis presented in Section 3.1, a maintenance model is developed to simulate the process of 2D chloride diffusion in repaired concrete structures exposed to a marine environment and estimate the extension of service life of RC structures under various repair strategies. In addition, this model assesses the ability of cover replacement measures to extend the long-term viability of the structure, therefore providing a method to compare model responses to different repair and maintenance strategies. The maintenance model assumes the structure has a service life of 75 years; the concrete has a water/cement ratio of 0.5 and consists of 400 kg/m^3 of Ordinary Portland Cement (OPC) with 8% C3A (cement tricalcium aluminate). The average ambient temperature and relative humidity are 15^{o}C and 0.70 respectively. The value of the time-invariant chloride concentration at the concrete surface, C_{fc}^{s}, is 6 kg/m^3, and the value of the critical chloride content at the reinforcement cover depth is 0.5% of the cement mass (C_{crit} = 2 kg/m^3). The quality and properties of the repair material are the same as those of the original concrete. The remainder of the parameters used in the model are listed in Table 1.
A square RC column with cross-sectional dimensions 0.4 m x 0.4 m is examined. It is subjected to chloride penetration in the two orthogonal directions x and y. The concrete cover depth, X_c, is 50 mm (as shown in Fig. 6)

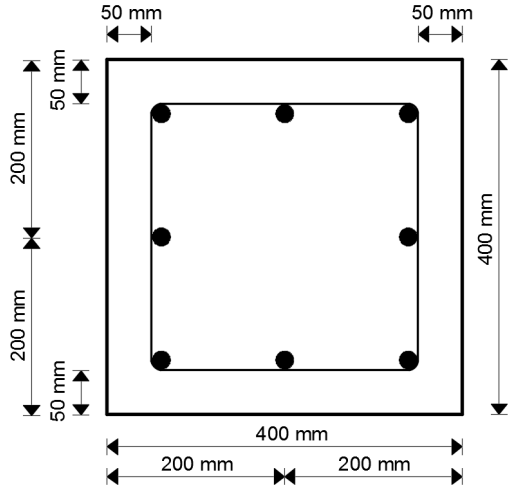

Fig. 6. Cross-sectional of square column

Exploiting the model symmetry, a 0.2 m x 0.2 m truncated model is developed, assuming that the reinforcing bars are not included in the model. Three concrete replacement strategies are simulated for the same structural element, including:

1. ORC1 strategy: Orthogonal concrete replacement with $X_p = X_c = 50$ mm, assuming that the repair thickness (X_p) is equal to the existing cover (Fig. 7a).
2. ORC2 strategy: Orthogonal concrete replacement with $X_p = 60$ mm > $X_c = 50$mm, where the repair thickness is assumed to be thicker than the existing cover (Fig. 7b)
3. CCR3 strategy: Circular concrete replacement where the boundary line between two materials is a circular curve (Fig. 7c)

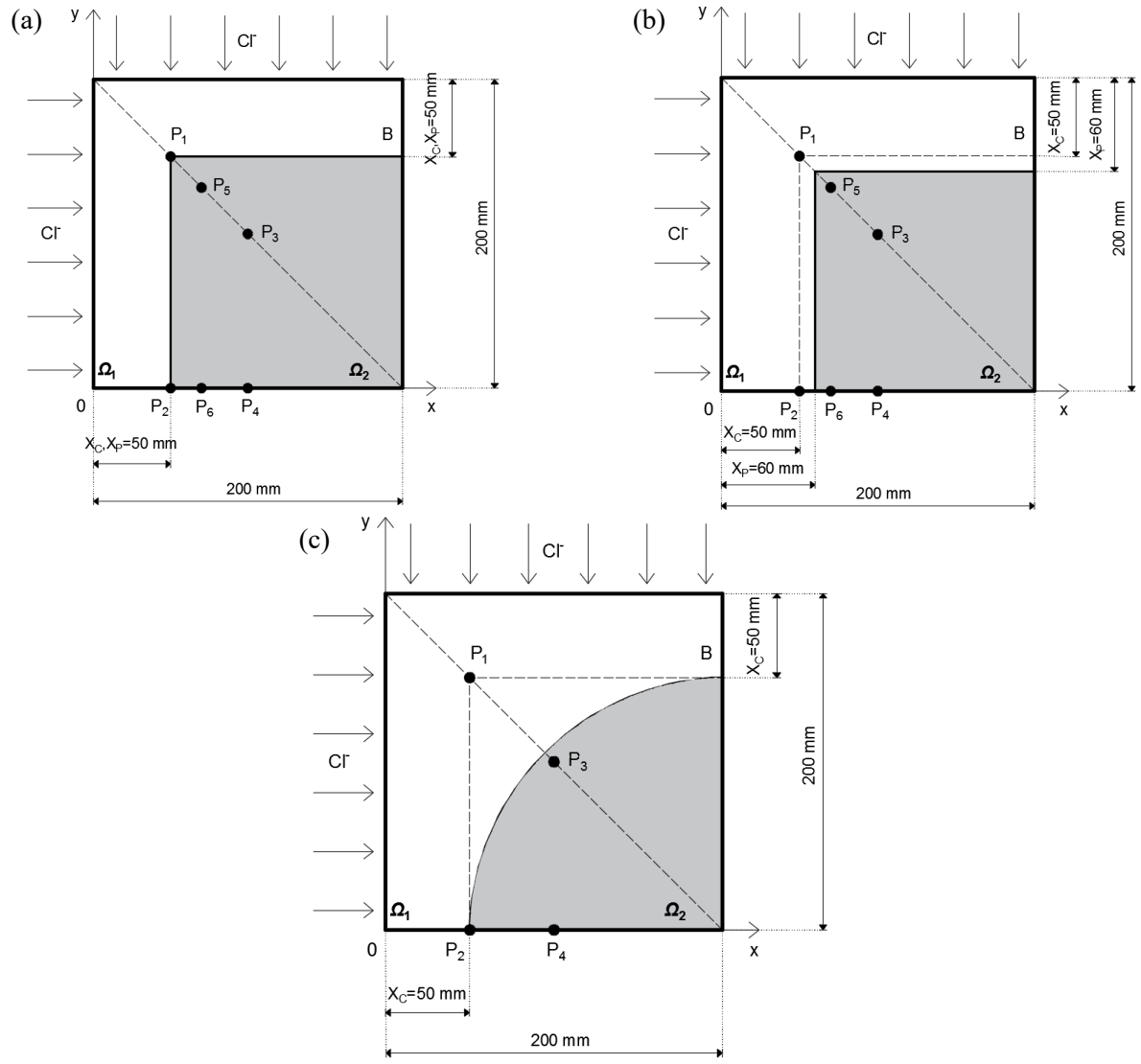

Fig. 7. (a) OCR1 with $X_p = X_c$, (b) OCR2 with $X_p > X_c$ (c) CCR3

3.3.2 Analysis of results

Under the reactive repair strategy, the corroded RC column is repaired by concrete replacement when the chloride content at the reinforcement cover exceeds a threshold that triggers corrosion. The maintenance model calculates the time intervals between repairs for the three strategies described above. Performing this analysis is necessary to a) understand the evolution of chloride concentration at different locations within the RC column elements, including the repaired material and original concrete, b) investigate how the shape and thickness of the concrete replacement affect the reduction of chloride concentration at critical locations, and c) define the maintenance schedule.

(a) Evolution of the chloride concentration within the repaired material

For each of the strategies OCR1, OCR2, and CCR3, the evolution of chloride concentration at two points located at the depth of the concrete cover was studied (as shown in Fig. 8). These points, designated P_1 and P_2, are depicted in Fig. 7 and have coordinates (0.05, 0.15) and (0.0.5, 0.0), respectively. Point P_1 corresponds to the chloride distribution at the corner reinforcement, while point P_2 represents the chloride distribution at a middle reinforcing bar.

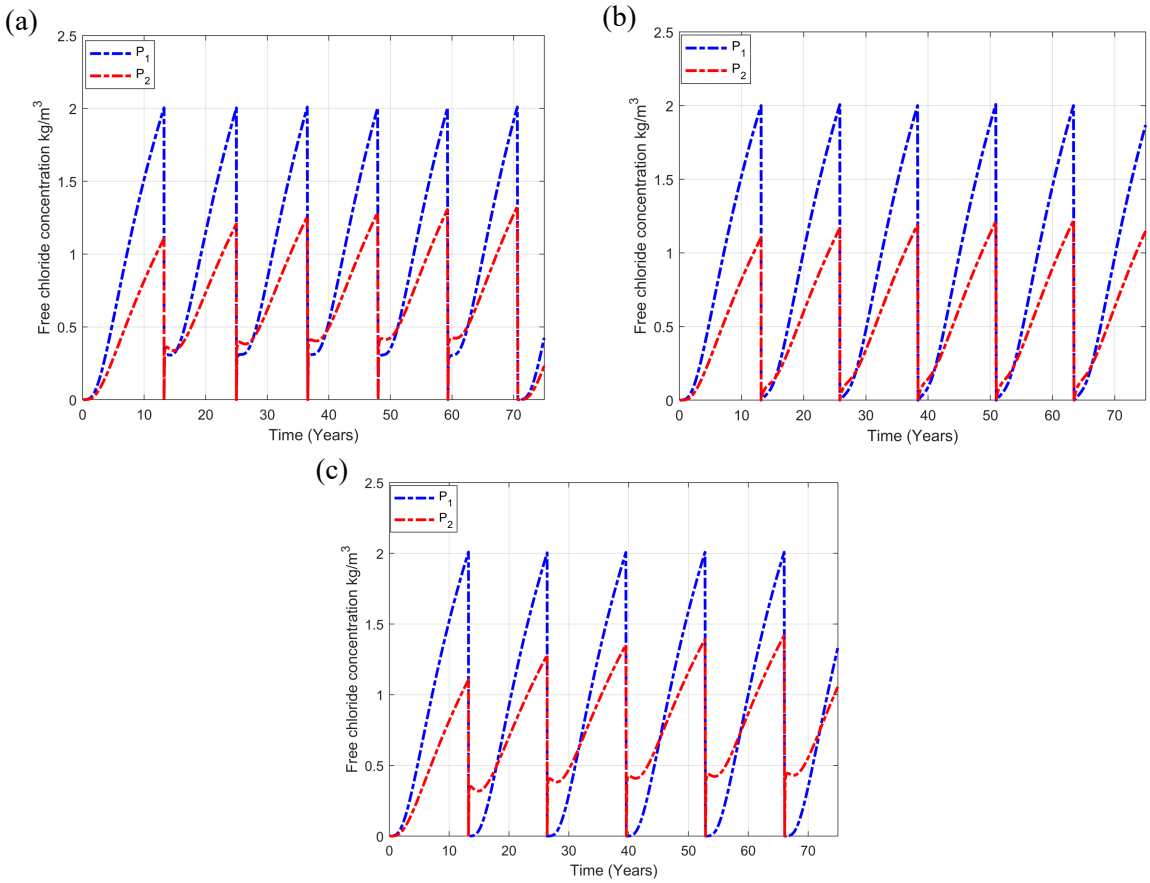

Fig. 8. The evolution of chloride concentration in different locations of repair concrete (a) OCR1, (b) OCR2 (c) CCR3

It is worth noting that if the repair thickness is equal to the existing cover (OCR1), the residual chloride in the old concrete quickly redistributes to points in the adjacent zone or to points at the critical depth, whereupon the redistribution is gradual (see Fig. 8a). A similar trend is observed for the chloride profile of point P_2 in CCR3 after repair (see Fig. 8c) because P_2 lies at the interface between Ω_1 and Ω_2, causing the chloride concentration at P_2 to predominate over P_1 in the initial years after repair. However, the chloride concentration at P_1 ultimately reaches C_{crit} before P_2 due to the increased uptake of environmental chloride at the corners of the element.

Thus, it can be seen that the chloride concentration accumulates to the critical value for the onset of corrosion at the corners (P_1) before it does at P_2, for all strategies (see the blue lines P_1 in Fig. 8a, b, c). This outcome is consistent with previous studies on corrosion in reinforced concrete (RC) structures subjected to two-dimensional chloride attack, which emphasize the corners of the concrete as the most crucial positions in predicting the time of corrosion initiation [16,39]. These results suggest that repair should occur when the chloride concentration reaches the critical threshold at point P_1 rather than at point P_2, as a delay in repair at this point may negatively impact the durability and serviceability of RC structures. To determine the time intervals between repairs for each strategy, Fig. 9 displays the progression of the chloride concentration at the corner of the square concrete column (P_1). It can be shown that the initial onset of corrosion occurs at approximately year 13 after the structure is put into service for all three strategies, as depicted by the blue line P_1 in Fig. 9. If the material properties of the structures prior to repair are kept constant, the determination of the first repair time is solely dependent on the thickness of the cover. On the other hand, the duration of subsequent repairs depends on the repair characteristics, particularly the shape and area of concrete removed. When the replacement concrete layer is thicker than the concrete cover (strategies OCR2 and CCR3), the time to corrosion initiation is longer than in strategy OCR1 (as shown in Fig. 9).

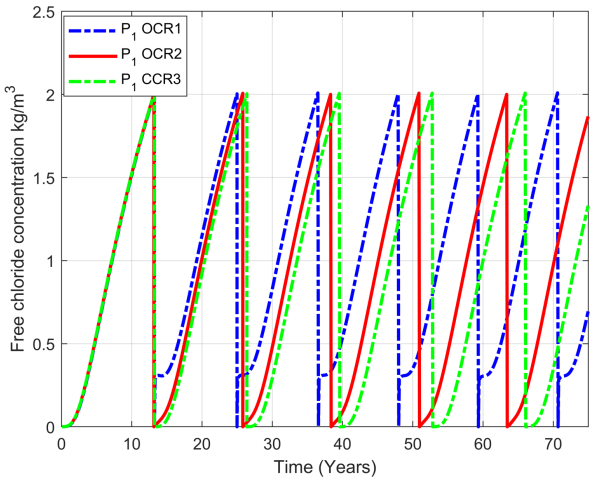

Fig. 9 The evolution of chloride concentration at the corner area in three strategies

Based on the results in Fig. 9, Table 2 shows the time intervals between corrosion occurrences during a 75-year service life, where the time interval between subsequent corrosion initiation times for OCR1 is about 11 years, while these time intervals for OCR2 and CCR3 are about 12.4 and 13 years, respectively. This can be explained by the fact that (1) there is a smaller amount of remaining concrete and thus fewer residual chloride ions in the old concrete layer, and (2) the position of P_1 in OCR1 is at the interface between Ω_1 (new concrete) and Ω_2 (old concrete with residual chloride ions) while in OCR2 and CCR3, P_1 belongs to the new concrete and is not in close proximity to the interface.

Table 2. Time intervals between corrosion occurrences for the three repair strategies

Strategy	Repair time (year)						
	1st	2nd	3rd	4th	5th	6th	7th
OCR1	13.15	11.67	11.42	11.26	11.17	11.1	$\Sigma T_i>75$
OCR2	13.15	12.57	12.41	12.41	12.32	12.32	$\Sigma T_i>75$
CCR3	13.15	13.06	13.06	13.06	13.06	$\Sigma T_i>75$	

To further support the aforementioned points, the profile of chloride concentration along the line P_1P_2 (as depicted in Fig. 7) at a depth corresponding to the concrete cover is plotted at three different time points, as shown in Fig. 10. Examining the blue curves in all three strategies (representing the chloride profile prior to repair at t = 13 years), it can be observed that the chloride concentration at the critical point P_1 is approximately equal to the threshold for the onset of corrosion, indicating the imminent need for repair. For the chloride profiles 10 years after the first repair (represented by the dashed yellow curves in Fig. 10a, b, c), the chloride concentration is highest at the corner and decreases towards the center of the element. At these time points, the mechanism of chloride transfer is no longer characterized by the redistribution of residual chloride in the old concrete, but rather by the penetration of chloride from the external environment. Among the three repair strategies, the chloride concentration at point P_1 is highest under OCR1 (about 1.7 kg/m^3), followed by OCR2 (about 1.6 kg/m^3), and lowest under CCR3 (about 1.5 kg/m^3). This suggests that, after the first repair, structures under the OCR1 strategy will require repair at the earliest point in time.

The chloride profile one year after repair in all three strategies (shown as dotted red curves in Fig. 10a, b, c) exhibits lower values because the concrete containing chloride was removed and replaced with a new layer of concrete. As the redistribution of residual chloride does not favor the corner location in the same manner as environmental chloride, the corner area does not display the highest chloride concentration one year after repair. Specifically, for the CCR3 strategy (involving a circular repair section, as depicted in Fig. 10c), the chloride concentration at point P_1 one year after repair is quite low and is largely unaffected by the redistribution of chloride ions from the old concrete. The observation

that the chloride concentration at P_1 is lower than at P_2 in the early years following repair under the CCR3 strategy aligns with the findings presented in Fig. 8c.

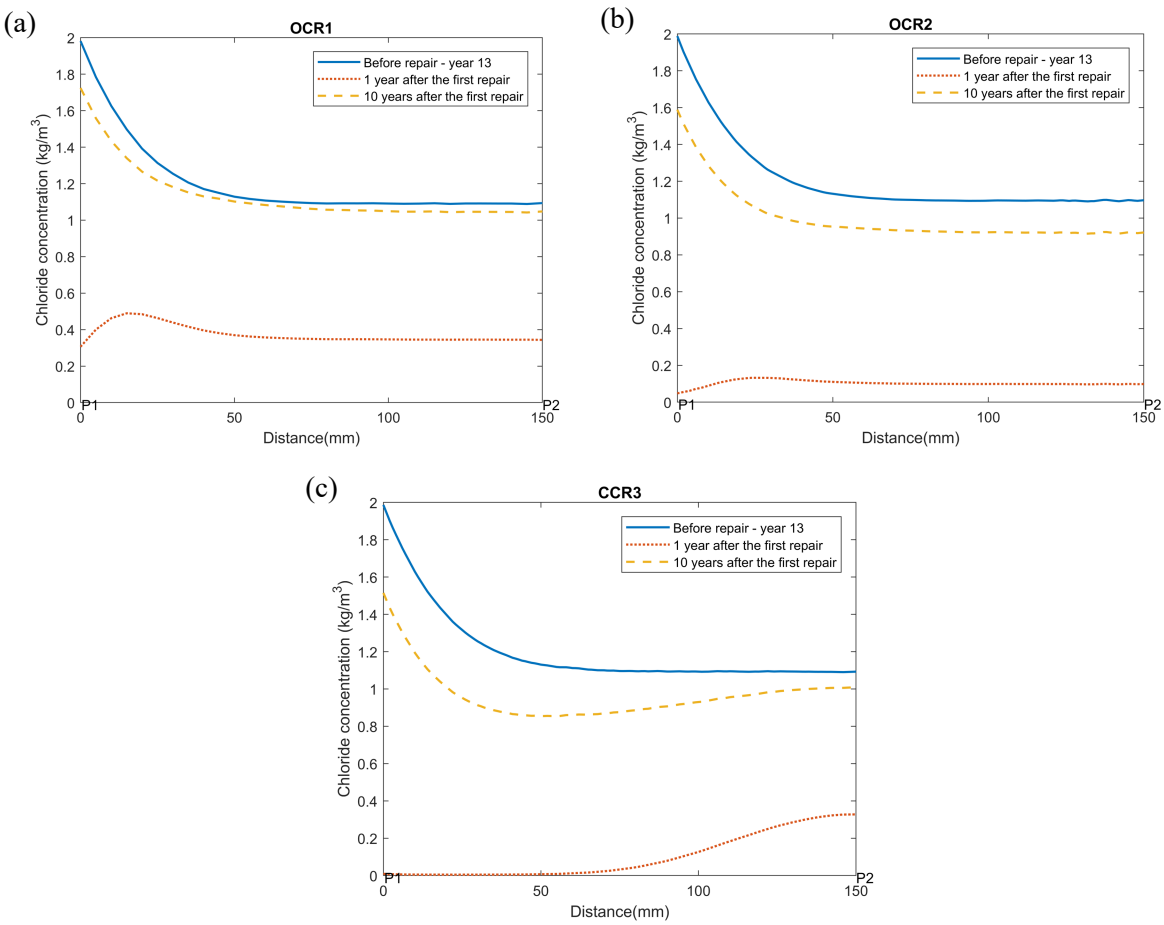

Fig. 10. The chloride concentration at the depth of concrete cover (a) OCR1, (b) OCR2 (c) CCR3

Fig. 11a, b, c depict iso-concentration contours of chloride ions (kg/m^3) one year following the initial repair, showcasing the redistribution of chloride ions at the boundary between aged and repaired concrete under the three strategies. In the orthogonal strategies (OCR1 and OCR2), residual chloride tends to accumulate in the corner regions after repair (Fig. 11a and Fig. 11b), while in the circular strategy (CCR3), where a larger amount of corner concrete has been replaced, the redistribution of chloride occurs initially near the center of each face of the element (Fig. 11c). This characteristic of CCR3 has proven advantageous in comparison to OCR2, which also replaces more concrete than the cover concrete layer, as it can help mitigate the buildup of chloride stresses in the corner regions and therefore extend the time until the onset of corrosion in these critical areas.

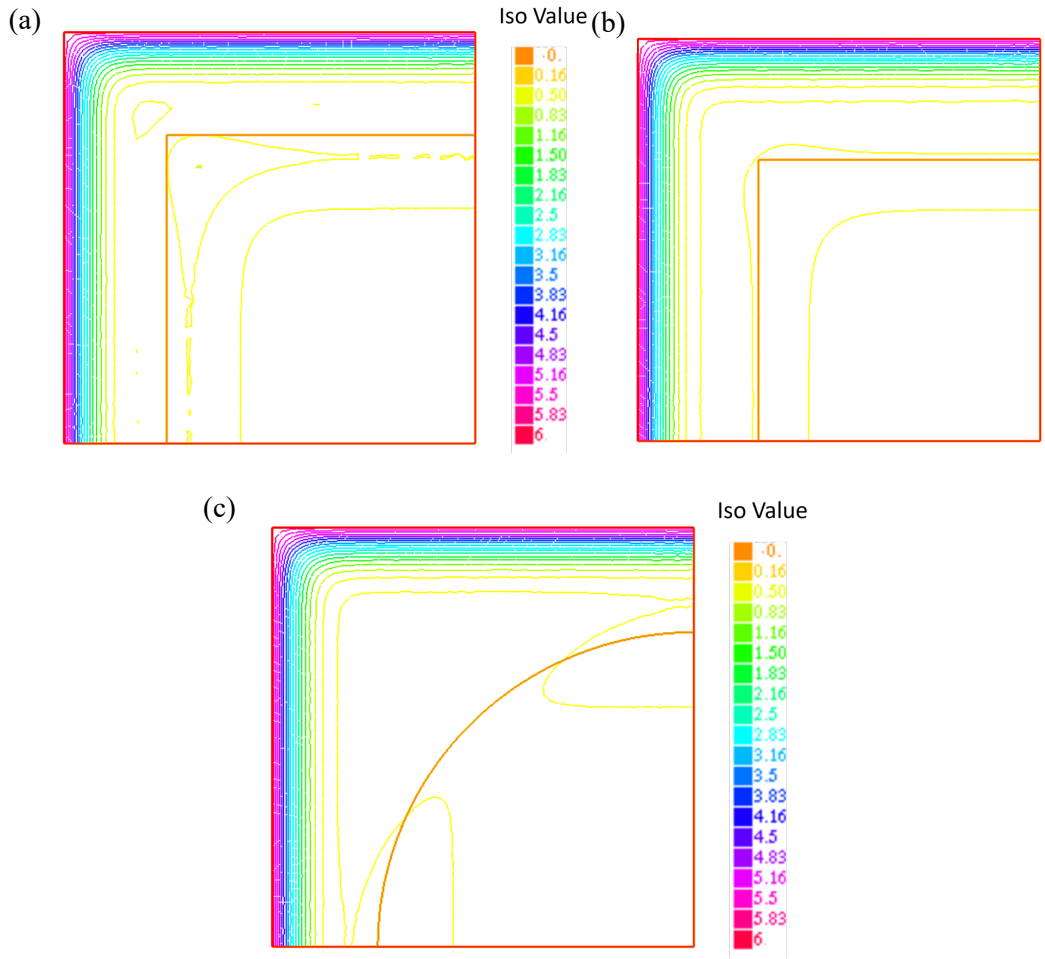

Fig. 11. Chloride ion iso-concentration contours at one year after the first repair (a) OCR1, (b) OCR2 (c) CCR3

(b) Evolution of chloride concentration in locations of unrepaired, aged concrete

Four points, designated P_3, P_4, P_5, and P_6 and located at coordinates (0.1, 0.1), (0.1, 0.0), (0.07, 0.13), and (0.07, 0.0), respectively (as depicted in Fig. 7), were studied for strategies OCR1 and OCR2. For strategy CCR3, only points P_3 and P_4 were examined. Point P_3 and P_5 are situated on the diagonal of the square cross-section of the concrete column, while points P_4 and P_6 are situated along the centerline of a face of the element and located within the old concrete, serving as representative points for areas that are distant from the corner area. The evolution of chloride concentration at these locations in the unrepaired, aged concrete is shown in Fig. 12a, b, c. These figures demonstrate a redistribution of the chloride ions remaining in the aged concrete after repair. For each repair strategy, the chloride concentration decreases immediately after repair due to the chloride absorption of the new concrete layer, and then gradually increases after a few years when redistribution is complete, and the environment is re-established as the primary source of chloride. This continues throughout the 75-year lifespan of the concrete structure, resulting in a curve that oscillates with the repair cycle, as shown in Fig. 12a, b, c. This oscillation is more pronounced at points that are closer to the repair boundary, such as P_5 and P_6 in strategies OCR1 and OCR2. At points far from the repair boundary, such as P_3 and P_4, the fluctuation is less pronounced because 1) there is less chloride at areas deeper beneath the element surface, and 2) there is no adjacent area of low chloride concentration to redistribute chloride ions to (see Fig. 12a, b). In strategy CCR3, the oscillation of chloride redistribution is also observed at point P_3 near the repair boundary, but it is not as pronounced as in strategies OCR1 and OCR2 (see line P_3 in Fig. 12c and P_5 in Fig. 12a, b). At point P_4, the chloride concentration gradually increases over time, surpassing the concentration at point P_3 after the first repair and then continuing to increase in subsequent years (see Fig. 12c). This trend is the opposite of that observed in strategies OCR1 and OCR2, where point P_3, near the corner of the element, consistently has a higher chloride concentration than the point near the middle of the column, point P_4 (see Fig. 12a, b).

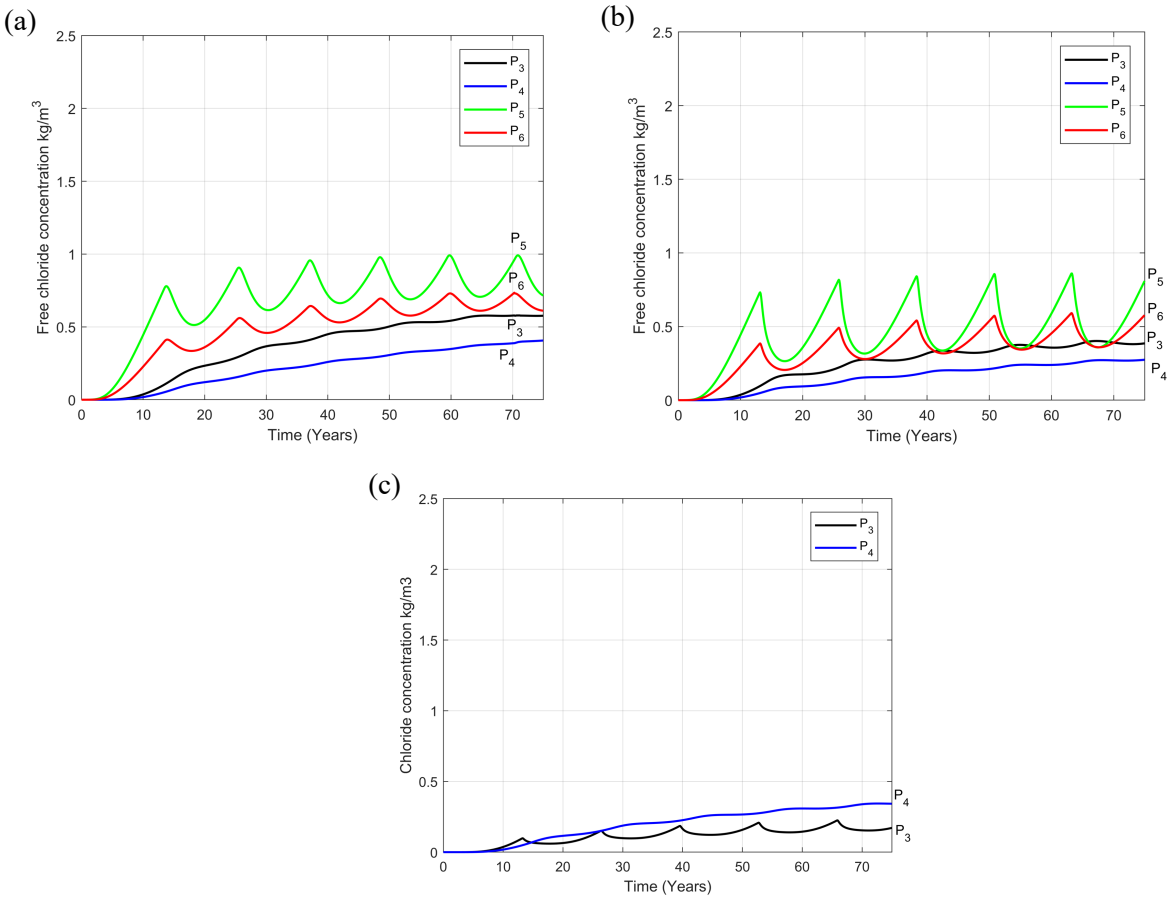

Fig. 12. The evolution of chloride concentration in different locations of unrepaired, aged concrete (a) OCR1, (b) OCR2, (c) CCR3

The findings from this study indicate that the CCR3 repair strategy, which employs a circular curve boundary rather than a vertical boundary, significantly impacts the distribution of residual chloride, resulting in a higher concentration in the central region compared to the corner region. Given that the corner of the concrete is typically identified as the most crucial location for predicting the onset of corrosion, the longer repair intervals of the CCR3 strategy, which translate to fewer repairs over the lifespan of the structure, can be attributed to this characteristic. Additionally, the replacement of new material leads to nearly zero chloride concentration at the location near the corner area immediately following repair, and the redistribution of chloride from the old concrete to this location is minimal. As a result, the CCR3 repair strategy has the potential to restore damaged structural elements to their original condition, with the time interval between corrosion outbreaks approaching the time to initial corrosion initiation. This is not observed in the repair of structures subjected to one-dimensional chloride attack [9,14] or in the CCR1 and CCR2 strategies, given that the quality and properties of the new concrete are assumed to be nominally identical to those of the original concrete.

(c) Maintenance schedule

As previously mentioned in Section 3.3.2(a), the outer column corners are the most crucial locations used for predicting the repair time of structures. When the onset of corrosion is considered as a repair criterion, the time intervals between corrosion occurrences in Fig. 9 and Table 2 indicate the times for repair based on a reactive approach. In practice, maintenance planning often follows a periodic schedule with predetermined repair times, resulting in preventative rather than reactive repairs. Therefore, this study proposes a periodic, preventative repair schedule, where repairs for each strategy are scheduled at annual intervals (as seen in Table 3).

In Table 3, the first preventative repair for all three strategies is scheduled 13 years after the structure is put into service. Subsequent to the initial repair, periodic repairs for OCR1, OCR2, and CCR3 are scheduled at repeating 11, 12, and 13-year intervals, respectively, throughout the remainder of the structure's service life. Repair strategies OCR2 and CCR3, which utilize thicker concrete replacement,

extend the time until the onset of corrosion and thus result in fewer repairs over the course of a structure's service life compared to strategy OCR1. Additionally, CCR3 is more effective than OCR2. Table 3 shows the number of repairs required during a 75-year service life for the three strategies OCR1, OCR2, and CCR3.

Table 3. Number of repairs for the three repair strategies

Strategy	Repair time (year)							Average number of repairs over 75 years*
	1st	2nd	3rd	4th	5th	6th	7th	
OCR1	13	24	35	46	57	68	>75	6.6
OCR2	13	25	37	49	61	73	>75	6.2
CCR3	13	26	39	52	65	>75		5.8

* Note: The decimal values are estimated by dividing the remaining life of the structure after the first repair by the respective repair interval specified for each strategy. The result of the above calculation plus the first repair is the expected number of repairs during the life of the structure. This approach allows us to avoid neglecting and underestimating the long-term effectiveness of different repair options and can be applied to structures with different expected lifetime assumptions.

For the purpose of simplicity, this study chooses to utilize simple orthogonal and curved repair sections. However, it is important to note that in practice, the repair characteristics should be optimized in order to achieve an optimal balance between the effectiveness of the repair and the volume of concrete replaced, which impacts cost, carbon dioxide (CO_2) emissions, and waste generation. The following section presents a comparison of the three strategies in terms of optimizing maintenance scheduling, cost, and environmental impact.

4 Repair and sustainable maintenance management

The main objective of this section is to propose a framework for comparing and selecting the best maintenance strategy among the three repair strategies discussed in Section 3.3, OCR1, OCR2, and CCR3. The proposed approach for the comparison between different repair alternatives that includes cost and environmental criteria is presented in Fig. 13. Due to different repair strategies in the form and thickness of replacement concrete, each strategy has a different long-term durability performance and service life extension profile. The maintenance schedule for each repair strategies is assessed using the methods described in section 3. With sustainability in mind, strict standards should apply to the repair and maintenance of concrete structures, both in terms of environmental impact and financial constraints [40]. A comparison of three factors could be used to assess the long-term feasibility of repair methods: cost, waste generation, and CO_2 emissions. These three criteria are afterwards computed for each maintenance schedule. Finally, the use of a multi-objective optimization approach is adopted to compare and select a sustainable maintenance solution.

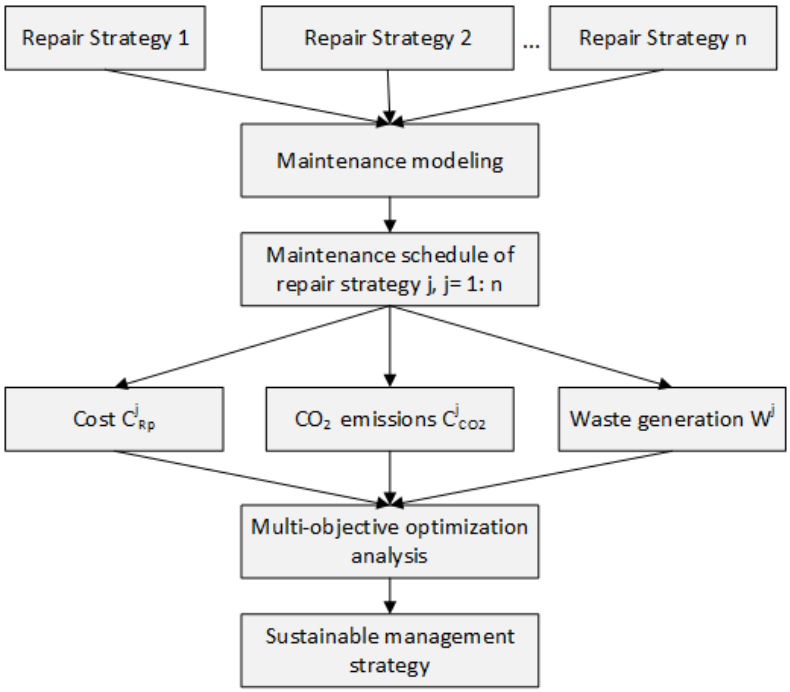

Fig. 13. Framework of sustainable maintenance management

4.1 Criteria and method for sustainable maintenance management

4.1.1 Costs

This study primarily relies on publicly available data on direct costs for comparing costs of the various repair strategies for deteriorating RC structures. Direct agency costs are limited to those associated with maintenance (inspection and repair). The analysis does not consider initial construction and residual costs because the study assumes repairs are made to identical RC components. Furthermore, each repair is assumed to be identical to the previous one.

According to [41], the cost of replacing concrete to cover depth, consisting of inspection, demolition, repair and operating loss, is C_{cover} = 323 €/m^2 (repair costs estimated for the port of Nantes-Saint-Nazaire in France). Excluding replacement of the corroded bars, the repair includes removal and reconstruction of corroded concrete cover between 4cm and 8cm for the damaged square cross section columns. The additional repair cost per mm of extra repair depth behind the cover is given in Table 4 [41] and accounts for the damage occurring on all four sides of the column. Consequently, the construction cost of one concrete replacement activity, C_t (€/m^2), is defined as:

$$C_t = C_{cover} + \text{Depth over cover (mm)} \times C_{extra} \quad (12)$$

It should be noted that repair costs can vary widely depending on specific installation conditions. Therefore, predicted results cannot be fully compared to other repair scenarios. However, it is possible to compare the life cycle costs of different repair strategies within the scope of this study.

Table 4. Extra repair costs for various structural columns

Structural element	Dimensions (mm)	C_{extra} (€/mm)
Square columns	300x300	1.56
Square columns	400x400	1.38
Square columns	600x600	1.01

Therefore, the total maintenance cost of each repair strategy (C_{RP}) over a structure's design lifespan is calculated as follows:

$$C_{RP} = C_t \times S_{RP} \times n_{RP} \quad (13)$$

where C_t is the construction cost of one repair activity at regular times over a service life period, S_{RP} is the surface area of the structure to be repaired, and n_{RP} is the number of repairs. It is assumed that the costs associated with a renewal, C_t, does not change over time and the discount rate is not considered.

4.1.2 CO_2 emissions

The environmental impact of concrete repair is classified into several categories [42]. In this study, the category of global warming impacts related to CO_2 emissions from cover replacement is examined. The six processes that affect the amount of CO_2 released are manufacturing of repair materials, transportation, water blasting to remove concrete cover, cleaning of reinforcement, protective coating of reinforcement, and application of shotcrete [25,42]. The estimated CO_2 emissions per cover repair measure are shown in the following table:

Table 5. CO_2 emissions per cover repair measure

Processes	CO_2 (kg CO_2 eq/m^3)	CO_2 (kg CO_2 eq/m^2)
Concrete Production	405	-
Hydro-jetting	-	84
Cleaning of reinforcement	-	22
Protective coating on reinforcement	-	1.4
Shotcrete application	-	4.4
Transportation	-	10
Total	405	121.8

It should be noted that the functional CO_2 units are not the same for all processes (as shown in Table 5). Therefore, the life cycle CO_2 emission (kg CO_2) for each repair strategy can be calculated as follows:

$$C_{CO_2} = (405\ V_{RP} + 121.8\ S_{RP})n_{RP} \quad (14)$$

where V_{RP} is the volume of concrete repaired, S_{RP} is the surface area of the structure to be repaired, and n_{RP} is the number of repairs.

4.1.3 Waste generation

Concrete demolition waste is 67% of global construction waste by weight (53% by volume) and only 5% is typically recycled. Waste generation (concrete waste) should be considered a criterion in sustainable assessment of repair and maintenance activities [40].

A comprehensive assessment would consider waste generated during actual repair and maintenance activities but also waste generated during the process of production of repair materials. However, because it is difficult to measure the waste generated during concrete production, this study only focuses on waste generated during repair work. The waste generated by cover replacement repair of $1m^3$ of concrete has been determined to be 1.3 m^3 of waste [43]. Therefore, the waste generation, $W(m^3)$, during the whole life cycle for each repair strategy, can be calculated from the repair volumes calculated in the repair analysis in this study as follows:

$$W = 1.3V_{RP} \times n_{RP} \quad (15)$$

where V_{RP} is the volume of concrete removed per cover replacement application, n_{RP} is the number of repairs of each repair strategy.

4.1.4 Methods for sustainable maintenance management

The complexity of multicenter management of deteriorating structures presents challenges for operating agencies of the facilities. Agencies have conflicting objectives to reduce costs, environmental impacts, and traffic disruptions while improving serviceability, functionality, and safety. A multi-objective optimization approach can help to solve these conflicts. This study considers the compromise programming approach, namely VIKOR [44]. The VIKOR approach allows the selection of a compromise solution with competing evaluation criteria. Ranking is based on similarity to an ideal alternative, where a compromise is defined as an agreement reached by mutual concessions, evaluating each alternative according to each criterion function. The L_p-metric, used as an aggregation function in a compromise programming approach, is the basis for the multi-criteria compromise ranking:

$$L_{p,j}=\left\{\sum_{i=1}^{n}\left[\frac{w_i\,(f_i^{*}-f_{ij})}{(f_i^{*}-f_i^{-})}\right]^{p}\right\}^{\frac{1}{p}},\ 1<p<\infty \qquad (16)$$

where f_{ij} is the value of the i^{th} criterion function for the alternative j; and f_i^* and f_i^- are the best and worst values of alternative j, respectively. n is the number of criteria, in this strategy there are three evaluation criteria: (1) costs, (2) CO_2 emission and (3) waste generation. w_i is the weight factor of the i^{th} criterion function, the value of w_i varies between 0 and 1 with $\Sigma w_i = 1$. The weight factors are subject to the operator's attitude towards each criterion.

$L_{1,j}$ (the value of S_i) and $L_{\infty,j}$ (the value of R_i) are used to formulate a ranking measure. S_j represents the maximum utility of alternative groups, while R_j stands for the least effective individual alternative. In addition, comprehensive indicator Q_j is used to rank the alternatives, where Q_j is the average weighted, normalized values S_j and R_j in the interval [0;1]. The VIKOR method is used to calculate the positive and negative points of the solution and finally the alternatives are ranked by sorting the values R, S, and Q in descending order. The alternative with the lowest value of Q is the best alternative. The steps to implement the VIKOR method and the conditions to achieve a compromise solution are well described in previous studies [44–46] and will not be presented here.

4.2 Selecting a sustainable maintenance strategy

4.2.1 Problem description and basic considerations

The purpose of this example is to show how the proposed methodology can be used to estimate the maintenance cost and environmental impact of a repair method and then choose the best compromise for a corroding structure. It is assumed that this structure (i.e., a harbor) consists of 86 RC column piles with a cross-section of 0.4 m x 0.4 m, placed in an aggressive marine environment and in need of repair during their 75-year lifespan. The total surface area of the structure to be repaired is about 400 m^2 for each maintenance procedure. The three maintenance strategies would perform one of OCR1, OCR2, and CCR3 repair exclusive throughout the structure's lifespan. The intervals between repairs are as shown in section 3.3.2 (c) and each satisfies the condition of reducing the risk of corrosion on the structure. Accordingly, the cost and environmental impact depend on the volume of concrete to be repaired and the number of repairs. To facilitate the calculation, the cost, CO_2 emissions, and waste generation are calculated per 1 m^2 of repaired concrete surface area, assuming damage on all four sides of the column.

The parameters used to estimate the maintenance cost and environmental impact of each repair strategy during the analysis period are shown in Table 6.

Table 6. Parameters for cost and environment impact assessment

Parameter	Value
Cross-sectional dimensions of concrete column	0.4 m x 0.4 m
Surface area of the structure to be repaired, S_{RP}	1 m^2
Volume of concrete repaired per one repair OCR1, V_{RP}^{OCR1}	0.04375 m^3
Volume of concrete repaired per one repair OCR2, V_{RP}^{OCR2}	0.051 m^3
Volume of concrete repaired per one repair CCR3, V_{RP}^{OCR3}	0.056 m^3
The number of repairs of OCR1	6.6
The number of repairs of OCR2	6.2
The number of repairs of CCR3	5.8
Maintenance Cost per one repair activity OCR1 (Repair thickness equal to the existing concrete cover)	323 €/m^2
Maintenance Cost per one repair activity OCR2 (Repair thickness 10 mm greater than existing concrete cover)	336 €/m^2
Maintenance Cost per one repair activity CCR3 (Repair thickness is converted to be 62 mm, 12 mm greater than existing concrete cover)	339 €/m^2

4.2.2 Results and discussion

Based on Eqs. (12)-(16) and Table 6, the calculated cost, CO_2 emissions, and waste generation for three repair strategies are placed in the decision matrix, as shown in Table 7.

Table 7. Decision Matrix

Alternatives	Cost (€/m^2)	CO_2 (kg CO_2)/m^3	Waste m^3
OCR1	852,720	368,320	150
OCR2	833,280	353,280	164.4
CCR3	786,480	335,200	168.8

It is noted in Table 7, that the repair method OCR1, with a lower repair thickness but a larger number of repairs, has the highest total maintenance cost of €852,720 and the highest CO_2 emissions for a 75-yer service life. The repair method CCR3, with the most damaged concrete removed but the least number of repairs, is the cheapest solution with a final cumulative cost of €786,480. In terms of environmental impact, CCR3 has the lowest CO_2 emissions but the highest waste generation due to a larger amount of concrete removed.

The VIKOR technique presented in Section 4.1.4 is used here to solve the multi-criteria decision-making problem and find the best compromised solution. Table 8 shows the ranking of the alternatives based on the S, R, and Q values, the description of which can be found in section 4.1.4. The best rank is assigned to the alternative with the smallest VIKOR value. These results were obtained by assuming that the agency assigns equal importance to costs and environmental impacts – i.e., w_{cost} = 0.5, w_{CO2} = 0.25 and w_{Waste} = 0.25 in Eq. (16).

Table 8. The ranking list for three repair strategies

	R value	Rank in R	S value	Rank in S	Q value	Rank in Q
OCR1	0.5	3	0.75	3	1	3
OCR2	0.353	2	0.681	2	0.638	2
CCR3	0.25	1	0.25	1	0	1

As a result, the repair strategy CCR3 is the selected alternative. The strategies OCR1 and OCR2, that follow the method of orthogonal concrete replacement, are not chosen because of their higher maintenance cost and larger environmental impact. Therefore, these repair methods are not recommended for corroded RC columns due to 2D chloride penetration. In addition, it is worth noting that when cost is weighted higher than 0.5, and total environmental factor therefore weighted less than 0.5, the VIKOR analysis leads to the same result, namely that CCR3 is the best option from the perspective of cost and environmental impact. Given these repair characteristics, the total number of repairs governs alternative selection.

5 Conclusions

This study develops a model for repair and maintenance of coastal RC structures exposed to 2D chloride attack. A degradation model that accounts for periodic repairs is used to predict the life extension of corroded RC structures and to evaluate the impact of maintenance actions on the long-term durability of the structures. Three repair strategies, namely orthogonal concrete replacement (strategies OCR1 and OCR2) and circular concrete replacement (strategy CCR3), are analyzed herein. The multi-criteria optimization approach VIKOR is then used to find a compromise solution based on three criteria: Cost, CO_2 emissions, and waste generation. The following conclusions can be drawn from the examples presented in this paper:

- The evaluation over time of chloride concentration in the corner areas of square/rectangular concrete sections is the most important indicator of time of corrosion onset during the service life of the structure.
- For long-term maintenance management, the circular concrete replacement strategy is recommended over orthogonal concrete replacement for repairing RC columns because it is more cost-effective and sustainable. Replacing a larger amount of corner concrete that follows a curved shape can help reduce the chloride concentration that accumulates in the corner region over time, extending the time for corrosion to begin.

- The effectiveness of different repair strategies in terms of concrete replacement shape and thickness can be compared by considering three factors, including cost, waste generation, and CO2 emissions. The results of the multi-criteria optimization analysis using the VIKOR method show that CCR3 is the most economical repair option and also the optimal solution for sustainable maintenance management.
- To the best knowledge of the authors, there are no previous experimental studies on RC structural elements exposed to two-dimensional chloride ingress and repaired using cover replacement techniques with different repair strategies. Consequently, no experimental data is currently available to compare and validate the repair model presented in this study. Further experiments are needed in the future for verification purposes and to investigate alternative repair materials.

Acknowledgements

This study was carried out in the framework of the Strengthening the Territory's Resilience to Risks of Natural, Climate and Human Origin (SIRMA) project, which is co-financed by the European Regional Development Fund (ERDF) through INTERREG Atlantic Area Program with application code: EAPA_826/2018. The sole responsibility for the content of this publication lies with the authors. It does not necessarily reflect the opinion of the European Union. Neither the INTERREG Europe program authorities are responsible for any use that may be made of the information contained therein.

References

[1] Bastidas-Arteaga E, Stewart MG. Damage risks and economic assessment of climate adaptation strategies for design of new concrete structures subject to chloride-induced corrosion. Struct Saf 2015;52:40–53. https://doi.org/10.1016/j.strusafe.2014.10.005.

[2] Ma Y, He Y, Wang G, Wang L, Zhang J, Lee D. Corrosion fatigue crack growth prediction of bridge suspender wires using Bayesian gaussian process. Int J Fatigue 2023;168:107377. https://doi.org/10.1016/j.ijfatigue.2022.107377.

[3] Tuutti K. Corrosion of steel in concrete. Swedish Cement and Concrete Research Institute, Stockholm., 1982.

[4] Qu F, Li W, Dong W, Tam VWY, Yu T. Durability deterioration of concrete under marine environment from material to structure: A critical review. J Build Eng 2021;35:102074. https://doi.org/10.1016/j.jobe.2020.102074.

[5] Bastidas-Arteaga E, Schoefs F. Stochastic improvement of inspection and maintenance of corroding reinforced concrete structures placed in unsaturated environments. Eng Struct 2012;41:50–62. https://doi.org/10.1016/j.engstruct.2012.03.011.

[6] Pritzl MD, Tabatabai H, Ghorbanpoor A. Laboratory Assessment of Select Methods of Corrosion Control and Repair in Reinforced Concrete Bridges. Int J Corros 2014;2014:1–11. https://doi.org/10.1155/2014/175094.

[7] Kharma KM, Ahmad S, Al-Osta MA, Maslehuddin M, Al-Huri M, Khalid H, et al. Experimental and analytical study on the effect of different repairing and strengthening strategies on flexural performance of corroded RC beams. Structures 2022;46:336–52. https://doi.org/10.1016/j.istruc.2022.10.078.

[8] BSEN 1504-10:2017, Products and Systems for the Protection and Repair of Concrete Structures-Definitions, Requirements, Quality Control and Evaluation of Conformity 2017.

[9] Truong QC, El Soueidy C-P, Li Y, Bastidas-Arteaga E. Probability-based maintenance modeling and planning for reinforced concrete assets subjected to chloride ingress. J Build Eng 2022;54:104675. https://doi.org/10.1016/j.jobe.2022.104675.

[10] Ma Y, Guo Z, Wang L, Zhang J. Probabilistic Life Prediction for Reinforced Concrete Structures Subjected to Seasonal Corrosion-Fatigue Damage. J Struct Eng 2020;146:04020117. https://doi.org/10.1061/(ASCE)ST.1943-541X.0002666.

[11] Skoglund P, Silfwerbrand J, Holmgren J, Trägårdh J. Chloride redistribution and reinforcement corrosion in the interfacial region between substrate and repair concrete—a laboratory study. Mater Struct 2008;41:1001–14. https://doi.org/10.1617/s11527-007-9301-6.

[12] Raupach M. Chloride-induced macrocell corrosion of steel in concrete—theoretical background and practical consequences. Constr Build Mater 1996;10:329–38. https://doi.org/10.1016/0950-0618(95)00018-6.

[13] Soleimani S, Ghods P, Isgor OB, Zhang J. Modeling the kinetics of corrosion in concrete patch repairs and identification of governing parameters. Cem Concr Compos 2010;32:360–8. https://doi.org/10.1016/j.cemconcomp.2010.02.001.

[14] Petcherdchoo A. Probability-Based Sensitivity of Service Life of Chloride-Attacked Concrete Structures with Multiple Cover Concrete Repairs. Adv Civ Eng 2018;2018:1–17. https://doi.org/10.1155/2018/4525646.

[15] Song H-W, Shim H-B, Petcherdchoo A, Park S-K. Service life prediction of repaired concrete structures under chloride environment using finite difference method. Cem Concr Compos 2009;31:120–7. https://doi.org/10.1016/j.cemconcomp.2008.11.002.

[16] Wu L, Wang Y, Wang Y, Ju X, Li Q. Modelling of two-dimensional chloride diffusion concentrations considering the heterogeneity of concrete materials. Constr Build Mater 2020;243:118213. https://doi.org/10.1016/j.conbuildmat.2020.118213.

[17] Liu Q, Sun L, Zhu X, Xu L, Zhao G. Chloride transport in the reinforced concrete column under the marine environment: Distinguish the atmospheric, tidal-splash and submerged zones. Structures 2022;39:365–77. https://doi.org/10.1016/j.istruc.2022.03.041.

[18] Ying J, Xiao J, Tam VWY. On the variability of chloride diffusion in modelled recycled aggregate concrete. Constr Build Mater 2013;41:732–41. https://doi.org/10.1016/j.conbuildmat.2012.12.031.

[19] Hu S, Peng J, Zhang J, Cai CS. Influences of Time, Temperature, and Humidity on Chloride Diffusivity: Mesoscopic Numerical Research. J Mater Civ Eng 2017;29:04017223. https://doi.org/10.1061/(ASCE)MT.1943-5533.0002080.

[20] Ababneh A, Benboudjema F, Xi Y. Chloride Penetration in Nonsaturated Concrete. J Mater Civ Eng 2003;15:183–91. https://doi.org/10.1061/(ASCE)0899-1561(2003)15:2(183).

[21] Anna V. Saetta RVS and Renato V Vitaliani. Analysis of Chloride Diffusion into Partially Saturated Concrete. ACI Mater J 1993;90. https://doi.org/10.14359/3874.

[22] Martín-Pérez B, Pantazopoulou SJ, Thomas MDA. Numerical solution of mass transport equations in concrete structures. Comput Struct 2001;79:1251–64. https://doi.org/10.1016/S0045-7949(01)00018-9.

[23] Bastidas-Arteaga E, Chateauneuf A, Sánchez-Silva M, Bressolette Ph, Schoefs F. A comprehensive probabilistic model of chloride ingress in unsaturated concrete. Eng Struct 2011;33:720–30. https://doi.org/10.1016/j.engstruct.2010.11.008.

[24] Bastidas-Arteaga E, Rianna G, Gervasio H, Nogal M. Multi-region lifetime assessment of reinforced concrete structures subjected to carbonation and climate change. Structures 2022;45:886–99. https://doi.org/10.1016/j.istruc.2022.09.061.

[25] Petcherdchoo A. Environmental Impacts of Combined Repairs on Marine Concrete Structures. J Adv Concr Technol 2015;13:205–13. https://doi.org/10.3151/jact.13.205.

[26] Binder F. Life cycle costs of selected concrete repair methods demonstrated on chloride contaminated columns. Th Int Probabilistic Workshop 2013:15.

[27] Bastidas-Arteaga E, Stewart MG. Cost-effective design to address climate change impacts. Eco-Effic. Repair Rehabil. Concr. Infrastruct., Elsevier; 2018, p. 613–36. https://doi.org/10.1016/B978-0-08-102181-1.00022-8.

[28] Wang Y, Gong X, Wu L. Prediction model of chloride diffusion in concrete considering the coupling effects of coarse aggregate and steel reinforcement exposed to marine tidal environment. Constr Build Mater 2019;216:40–57. https://doi.org/10.1016/j.conbuildmat.2019.04.221.

[29] Zacchei E, Bastidas-Arteaga E. Multifactorial Chloride Ingress Model for Reinforced Concrete Structures Subjected to Unsaturated Conditions. Buildings 2022;12:107. https://doi.org/10.3390/buildings12020107.

[30] Li Y, Fu Z, Tan P, Shang J, Mi P. Life cycle resilience assessment of RC frame structures considering multiple-hazard. Structures 2022;44:1844–62. https://doi.org/10.1016/j.istruc.2022.08.092.

[31] Hecht F. New development in freefem+. J Numer Math 2012;20:251–65. https://doi.org/10.1515/jnum-2012-0013.

[32] Petcherdchoo A, Chindaprasirt P. Exponentially aging functions coupled with time-dependent chloride transport model for predicting service life of surface-treated concrete in tidal zone. Cem Concr Res 2019;120:1–12. https://doi.org/10.1016/j.cemconres.2019.03.009.

[33] Stephen L. Amey DAJ Matthew A Miltenberger, and Hamid Farzam. Predicting the Service Life of Concrete Marine Structures: An Environmental Methodology. ACI Struct J 1998;95. https://doi.org/10.14359/540.

[34] Yu B, Ling G, Fan Z, Chen Z, Yang L. Numerical modelling and experimental validation of two-dimensional chloride concentration distribution within concrete. Constr Build Mater 2021;298:123804. https://doi.org/10.1016/j.conbuildmat.2021.123804.

[35] Wu L, Wang Y, Wang Y, Ju X, Li Q. Modelling of two-dimensional chloride diffusion concentrations considering the heterogeneity of concrete materials. Constr Build Mater 2020;243:118213. https://doi.org/10.1016/j.conbuildmat.2020.118213.

[36] Wang Y, Liu C, Wang Y, Li Q, Liu H. Time-and-Depth-Dependent Model of Chloride Diffusion Coefficient for Concrete Members Considering the Effect of Coarse Aggregate. J Mater Civ Eng 2018;30:04017302. https://doi.org/10.1061/(ASCE)MT.1943-5533.0002161.

[37] Roy SK, Liam Kok Chye, Northwood DO. Chloride ingress in concrete as measured by field exposure tests in the atmospheric, tidal and submerged zones of a tropical marine environment. Cem Concr Res 1993;23:1289–306. https://doi.org/10.1016/0008-8846(93)90067-J.

[38] Alabduljabbar H, West J. Bond behavior of cleaned corroded rebar repaired by partial depth repair. Structures 2020;27:813–23. https://doi.org/10.1016/j.istruc.2020.06.022.

[39] Jin L, Zhang R, Du X, Li Y. Investigation on the cracking behavior of concrete cover induced by corner located rebar corrosion. Eng Fail Anal 2015;52:129–43. https://doi.org/10.1016/j.engfailanal.2015.03.019.

[40] Bastidas-Arteaga E, Schoefs F. Sustainable maintenance and repair of RC coastal structures. Proc Inst Civ Eng - Marit Eng 2015;168:162–73. https://doi.org/10.1680/jmaen.14.00018.

[41] Bastidas-Arteaga E, Stewart MG. Climate adaptation of existing reinforced concrete structures in coastal areas. XIIIèmes JNGCGC Dunkerque, Editions Paralia; 2014, p. 629–40. https://doi.org/10.5150/jngcgc.2014.069.

[42] Årskog V, Fossdal S, Gjørv OE. LIFECON DELIVERABLE D 5.3 Methodology and data for calculation of LCE (Life Cycle Ecology) in repair planning. n.d.

[43] Bastidas-Arteaga E. Contribution for sustainable management of reinforced concrete structures subjected to chloride penetration. n.d.

[44] San Cristóbal Mateo JR. Multi Criteria Analysis in the Renewable Energy Industry. London: Springer London; 2012. https://doi.org/10.1007/978-1-4471-2346-0.

[45] Mardani A, Zavadskas E, Govindan K, Amat Senin A, Jusoh A. VIKOR Technique: A Systematic Review of the State of the Art Literature on Methodologies and Applications. Sustainability 2016;8:37. https://doi.org/10.3390/su8010037.

[46] Mateusz P, Danuta M, Małgorzata Ł, Mariusz B, Kesra N. TOPSIS and VIKOR methods in study of sustainable development in the EU countries. Procedia Comput Sci 2018;126:1683–92. https://doi.org/10.1016/j.procs.2018.08.109.